Fernanda Cristina de Moraes Takafuji
e-mail: fernanda.takafuji@gmail.com

Clóvis de Arruda Martins
e-mail: cmartins@usp.br

Department of Mechanical Engineering,
Av. Prof. Mello Moraes, 2231,
University of São Paulo,
05508-970 São Paulo, SP, Brazil

Comparison Between Frequency Domain and Time Domain Riser Analysis

In the optimization or parametric analyses of risers, several configurations must be analyzed. It is laborious to perform time domain solutions for the dynamic analysis, since they are time-consuming tasks. So, frequency domain solutions appear to be a possible alternative, mainly in the early stages of a riser design. However, frequency domain analysis is linear and requires that nonlinear effects are treated. The aim of this paper is to present a possible way to treat some of these nonlinearities, using an iterative process together with an analytical correction, and compare the results of a frequency domain analysis with the those of a full nonlinear analysis. [DOI: 10.1115/1.4006149]

1 Introduction

Risers are elements that connect the oil well, at the sea bottom, to the floating production unit. They are susceptible to loads caused by ocean currents and waves. The global analysis aims to study the riser behavior due to those environmental loads. This is an essentially nonlinear problem, since it includes large displacements, unilateral contact, and nonlinear viscous damping loads.

The structural analysis can be divided into two stages: static analysis and dynamic analysis. For riser analyses, the static one considers the loads that are time independent: weight, buoyancy, and current loads. Although the current's velocity profile varies with time, its scale of variation is substantially greater than the first natural period of the riser and, therefore, it can be considered constant. The dynamic analysis includes wave loads and the movement induced at the riser's top by the floating unit.

To take into account all the nonlinearities of the problem, the dynamic analysis must be performed in the time domain. It means that the response is calculated for every time step and the simulation time depends on the time that the transient response takes to die away. To achieve convergence, the time step must be small and, for that reason, a time domain analysis could take a long time.

To choose the most suitable configuration for a given application, in the first stages of a riser design, several configurations must be simulated through a parametric analysis or optimization methods. Frequency domain solutions appear as an alternative to considerably reduce the time spent in dynamic analyses however, to implement them, all of the nonlinearities have to be treated or removed somehow.

The purpose of this work is to present a possible way to address the nonlinearities inherent in the analysis of risers, concluding that frequency domain analysis can give similar results to the ones obtained with a time domain analysis for harmonic seas. To achieve this purpose some results of a case study, obtained with both methods, were compared. Two different configurations were considered: free-hanging and lazy-wave.

The analyses in the time domain were performed using Orcaflex™ version 9.4a; see Ref. [1] for further information. The frequency domain analyses were performed using in-house software whose model and linearization process are presented in this paper.

Despite its importance, vortex-induced vibration (VIV) is beyond the scope of this work and will not be considered in the models presented here. Methods of transformation of real (random) sea states into harmonic sea states will also not be discussed in this paper.

2 Modeling

2.1 Static. The aim of the static analysis is to find the static balance configuration and the forces and moments acting on the riser when it is subjected to time-invariant loads.

Although this work focuses on the dynamic analysis, the static configuration is important since it can be used as the initial configuration of the dynamic analysis and in the frequency domain the dynamic response is considered to be a perturbation of this configuration. There are many different ways to perform the static analysis. Patel and Seyed [2] provide a wide-ranging bibliography on this topic. A good approximation of the static solution can be obtained with the catenary equations, which consider the weight and buoyancy, but no bending stiffness. Other approaches include the bending stiffness and other effects. Since the focus of this work is on the dynamic solution, any approach could be used to obtain the static configuration. The solution that is briefly described next is the one used here.

The static model is based on the model presented in Santos [3]. This reference is in Portuguese, but Silveira and Martins [4] present a similar numerical solution for two-dimensional problems and Silveira and Martins [5] show a solution for three-dimensional ones.

The static loads considered in that work are: weight, buoyancy, and drag caused by the sea water current, which is considered constant in time, since the time scale of the variation of the mean velocity of the current is substantially greater than the first natural period of the riser. The riser is initially modeled without the bending stiffness, which causes a discontinuity of the curvature in the touchdown point (TDP) and top regions. Since this discontinuity is not real, it is removed afterwards through a boundary layer technique, as presented in Aranha et al. [6]. The seabed is considered plain, horizontal, and rigid.

Risers with different segments can be analyzed considering that the mechanical properties are constant within each segment. The axial stiffness is included and it is assumed that the riser's material is always in the elastic regime.

The differential equations that describe the static behavior of the riser are then obtained. The boundary conditions are: the position where the riser is connected on the float unit is known, the position of the other extreme coincides with the origin of the coordinate system, and the vertical coordinate $z = 0$ at the TDP, however, the curvilinear coordinate s at the TDP is unknown. The static analysis consists of obtaining the solution of the differential equations considering the boundary conditions. However, since

Contributed by the Ocean Offshore Mechanics and Arctic Engineering Division of ASME for publication in the JOURNAL OF OFFSHORE MECHANICS AND ARCTIC ENGINEERING. Manuscript received August 16, 2010; final manuscript received October 10, 2011; published online May 30, 2012. Assoc. Editor: Daniel T. Valentine.

the boundary conditions are known for more than one position, the integration could be started at the anchor or at the top using a shooting method, as described by Keller [7].

The numerical integration of the differential equations is performed through a 3-4 Runge-Kutta method, with an adaptive step. This method was used in Martins [8] and the step is inversely proportional to the curvature. Further information on the model, ordinary differential equations, and numerical integration can be found in [3–5].

2.2 Dynamic. There are different ways to dynamically analyze the riser. The model used in this work is briefly described next. However, the linearization methods presented in the next section could be used with different models as well.

The dynamic loads considered in this work are: drag caused by waves and sea current and the prescribed movement of the floating unit. Part of the drag force caused by the current has already been considered in the static analysis. However, the drag force caused by the waves, along with the combined effect of the wave and the current, is considered in the dynamic analysis.

Besides the hypotheses considered in the static analysis, it is also assumed here that the dynamic loads are harmonic. Thus, the amplitude and period of the waves are known and the float unit's motion is prescribed through amplitudes and phases relative to the wave. The period of the prescribed motion is considered to be the same as the wave's. The static configuration is not updated during the dynamic simulation and the dynamic response is assumed to be a perturbation of the static configuration.

The solution is numerically obtained through the finite element method. The riser is represented by Euler-Bernoulli beams and the equation that governs its dynamics is

$$M\ddot{q}(t) + C(\dot{q}(t))\dot{q}(t) + K(q(t))q(t) = p(\dot{q}(t)) \tag{1}$$

where M is the mass matrix including the effect of the additional mass, $C(\dot{q}(t))$ is the damping matrix, which depends on the riser velocity, K is the elastic and geometric stiffness matrix and $p(\dot{q}(t))$ is the external load. Here, $\ddot{q}$, $\dot{q}$, and q are the acceleration, velocity, and displacement vectors of the structure, respectively. All of the global matrices depend on the position of the riser at every time step.

We consider a harmonic surface wave, traveling in deep water. One of the extremities of the riser is connected to the floating unit, which moves as the waves go by. The motion is transmitted to the top, making the whole riser move.

Different from the time domain analysis, where the criteria used to obtain the wave velocity above the mean wave level is to consider that it is the same velocity of the particles at the mean wave level, in the frequency domain, it is assumed that the particle's velocity above the mean wave level is zero.

3 Linearization

3.1 Linearization of Rotation and Stiffness. One of the nonlinear effects inherent in the dynamic analysis of risers concerns the geometrical stiffness matrix. It depends on the tension of the elements, which changes dynamically. In addition, so does the position of the riser, which should be known at each time step in order to rotate all of the elements' matrices to form the global ones.

To treat both nonlinearities, we consider that the dynamic response is a perturbation of the static configuration, thus, it is assumed that the matrices do not change during the analysis.

3.2 Linearization of Damping. In this section, a linearization method for the viscous damping will be presented. The viscous part of Morison's formula, presented in Morison et al. [9], is a quadratic equation in the relative velocity, as is shown next

$$\vec{f}_{D,t} = -\frac{1}{2}\rho_a D C_{D,t} \left|\vec{v}_{m,t} - \vec{v}_{c,t}\right| \left(\vec{v}_{m,t} - \vec{v}_{c,t}\right) \tag{2}$$

where $\vec{v}_m$ is the relative velocity between the riser's velocity $\dot{q}$ and the wave's velocity $\vec{v}_w$, $\vec{v}_c$ is the current velocity, D is the riser's diameter, C_D is the drag coefficient, ρ_a is the fluid density, and the index t is related to the transversal direction.

There are many ways to treat this nonlinear effect for the frequency domain analysis. The first works concerning the linearization of drag forces were performed in two dimensions. In this case, the problem can be treated as a scalar, as observed by Dantas et al. [10]. One example is the work of Gudmestad and Connor [11], where the approximation $|v_w - \dot{q}| \cdot (v_w - \dot{q}) \approx |v_w| \cdot (v_w - \dot{q})$ is considered and the linear form is obtained from a least squares approximation.

Langley [12] presents a three-dimensional linearization through the minimization of the mean squared error and Leira [13] compares different methods of linearization. Chen and Lin [14] propose using a Fourier expansion up to any nth order.

Liu and Bergdahl [15] propose a linearization method where the work done by the motion of the cable in the time domain is equated to the work in the frequency domain. This is similar to the method presented in Martins [16] for two dimensional problems.

In the method presented in Martins [16], only one linearization coefficient is used for the whole riser. Takafuji and Martins [17] extended that work, proposing that one coefficient is used for each element. That method was extended in Takafuji [18] for three-dimensional cases using one coefficient per element for the transversal force. According to Teng and Li [19], if only one coefficient is used, the linearized drag force can be too large in one direction and too small in the other one. Therefore, they suggested the use of two coefficients per element and that will be used in this work as well.

The suggested methodology is based on maintaining the dissipated energy in one cycle. The coefficients depend on the relative velocity between the fluid and the riser, which is unknown at the beginning of the analysis. For that reason, the coefficients are iteratively obtained. The iterative process is necessary to take into account, as closely as possible, the nonlinearity caused by Morison's formula.

In the three-dimensional problem, the riser does not have one transversal direction, as in the two-dimensional one. It has a transversal plane instead, which changes along the length. For this reason, the linearization force is placed in a fixed base $\left(\vec{i},\vec{j},\vec{k}\right)$, with the origin on the anchor.

Next, we describe how the linear expression for the transversal direction is obtained. The linear expression for the axial direction is obtained in an analogous way.

The viscous part of Morison's formula for the dynamic analysis in the transversal direction is given by

$$\begin{aligned}\vec{f}_{D,t} = &-\frac{1}{2}\rho_a D C_{D,t} \left|\vec{v}_{m,t} - \vec{v}_{c,t}\right| \left(\vec{v}_{m,t} - \vec{v}_{c,t}\right) \\ &-\frac{1}{2}\rho_a D C_{D,t} \left|\vec{v}_{c,t}\right| \left(\vec{v}_{c,t}\right)\end{aligned} \tag{3}$$

The first part of Eq. (3) corresponds to the total force and the second part corresponds to the force caused by the current that has already been considered in the static analysis.

To solve the problem in the frequency domain, it is necessary that the dynamic damping force is approximated to a harmonic force. Considering that $\vec{v}_{m,t}$ is harmonic, one can write a linearized damping force as

$$\vec{\tilde{f}}_{D,t} = -\frac{1}{2}\rho_a D C_{D,t} \cdot \begin{bmatrix} K_{t1} & 0 \\ 0 & K_{t2} \end{bmatrix} \cdot \begin{bmatrix} \vec{v}_{m,t1} \\ \vec{v}_{m,t2} \end{bmatrix} \tag{4}$$

where K_{t1} is the linearization coefficient in transversal direction $\vec{t}_1$ and K_{t2} is the linearization coefficient in the other transversal

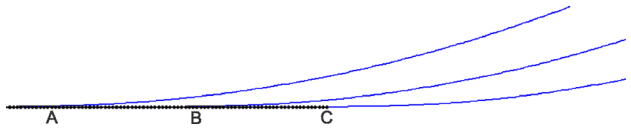

Fig. 1 Sketch of the TDP movement. The middle position B is the static configuration and the other two, A and C, are dynamic instants. The black dots represent the seabed.

direction $\vec{t}_2$. Here, $\vec{t}_1$ and $\vec{t}_2$ are orthogonal vectors that define the transversal plane. In addition, the indexes t_1 and t_2 are related to the directions $\vec{t}_1$ and $\vec{t}_2$.

However, the coefficients K_{t1} and K_{t2} are not known at the beginning of the analysis and their values have to be estimated. Since the main purpose of the damping is energy dissipation, the chosen criteria to find an equivalent linear expression is to keep the dissipated energy in one cycle with period T. It means to impose that

$$\int_0^T \vec{f}_{D,ti} \cdot \dot{\vec{q}}_t dt = \int_0^T \vec{\tilde{f}}_{D,ti} \cdot \dot{\vec{q}}_t dt \tag{5}$$

where the index i can be direction 1 or 2.

Substituting Eqs. (3) and (4) into Eq. (5) leads to

$$\int_0^T \left(|\vec{v}_{m,t} - \vec{v}_{c,t}|(\vec{v}_{m,ti} - \vec{v}_{c,ti}) + |\vec{v}_{c,t}|\vec{v}_{c,ti}\right)\dot{\vec{q}}_t \cdot dt = K_{ti}\int_0^T \vec{v}_{m,ti} \cdot \dot{\vec{q}}_t \cdot dt \tag{6}$$

The relative velocity between the riser and the wave can be written in the base $\left(\vec{i},\vec{j},\vec{k}\right)$ in the harmonic way

$$\vec{v}_{m,t} = A_x\omega \cdot \sin(\omega t + \phi_x)\vec{i} + A_y\omega \cdot \sin\left(\omega t + \phi_y\right)\vec{j} + A_z\omega \cdot \sin(\omega t + \phi_z)\vec{k} \tag{7}$$

where $\omega = 2\pi/T$. The velocity of the riser in the harmonic way can be written as

$$\dot{\vec{q}}_t = C_x\omega \cdot \sin(\omega t + \varphi_x)\vec{i} + C_y\omega \cdot \sin\left(\omega t + \varphi_y\right)\vec{j} + C_z\omega \cdot \sin(\omega t + \varphi_z)\vec{k} \tag{8}$$

Additionally, the current velocity can be written as

$$\vec{v}_{c,t} = V_{t,x}\vec{i} + V_{t,y}\vec{j} + V_{t,z}\vec{k} \tag{9}$$

Inserting Eqs. (7), (8), and (9) into Eq. (6), isolating K_{ti}, and considering that

$$\int_0^T \sin(\omega t + k)dt = 0$$

and

$$\int_0^T \sin(\omega t + k_1) \cdot \sin(\omega t + k_2)dt = \frac{\pi}{\omega}\cos(k_1 - k_2)$$

One can obtain

$$K_{ti} = \frac{I_1}{I_2} \tag{10}$$

where

$$I_1 = \int_0^T \Big(\left(A_x\omega \sin(\omega t + \phi_x) - V_{t,x}\right)^2 + \left(A_y\omega \sin\left(\omega t + \phi_y\right) - V_{t,y}\right)^2 + \left(A_z\omega \sin(\omega t + \phi_z) - V_{t,z}\right)^2 \Big)^{1/2} \left[\left(A_{xi}\omega \sin(\omega t + \phi_{xi}) - V_{t,xi}\right)C_x\omega \sin(\omega t + \varphi_x) + \left(A_{yi}\omega \sin\left(\omega t + \phi_{yi}\right) - V_{t,yi}\right)C_y\omega \sin\left(\omega t + \varphi_y\right) + \left(A_{zi}\omega \sin(\omega t + \phi_{zi}) - V_{t,zi}\right)C_z\omega \sin(\omega t + \varphi_z)\right] \cdot dt$$

and

$$I_2 = \pi\omega\left(A_{xi}C_x \cos(\phi_{xi} - \varphi_x) + A_{yi}C_y \cos\left(\phi_{yi} - \varphi_y\right) + A_{zi}C_z \cos(\phi_{zi} - \varphi_z)\right)$$

3.3 Linearization of the Riser-Seabed Contact. Another nonlinearity that should be treated for the frequency domain analysis is the riser-soil contact. During the dynamic analysis, the TDP changes as the floating unit moves, as shown in Fig. 1.

To remove that nonlinear effect in this model, the static TDP is replaced by a pinned support and only the suspended part of the riser is dynamically analyzed, as Fig. 2 shows.

That might affect the results at the TDP region, especially the curvature, since a peak that generally appears in the contact region does not appear.

One way to recover this peak is to apply a boundary layer technique. It is applied to correct the curvature corresponding to the angle θ, the angle formed between the riser and the horizontal plane, because of the contact with the seabed. In the ψ direction, which is angle formed between the riser and the x-axis, there is no nonlinear contact condition.

3.4 Boundary Layer. Based on a model presented in Aranha et al. [6], this technique is applied after the frequency domain analysis is performed, once some results at the TDP are required for this analysis.

The curvature is corrected through an asymptotical solution, since the effect of the TDP motion is restricted to the TDP region.

The curvature can be written as

$$\chi(s,t) = \frac{1}{2}\left((1 + \text{signal}\,\beta_{CL}(s,t))(1 - e^{-\beta_{CL}(s,t)})\right)\chi_{0,TDP} \tag{11}$$

where $\chi_{0,TDP}$ is the static curvature at the TDP

$$\beta_{CL}(s,t) = \frac{s - s_{TDP} - x_0(t)}{\hat{\lambda}}$$

$$\hat{\lambda}(t) = \sqrt{\frac{EI}{T_{ef,0}}}.\left(1 + \frac{T_{din}(t)}{T_{ef,0}}\right)^{-1/2}$$

Here, EI is the bending stiffness of the riser, $T_{ef,0}$ is the static effective tension at the TDP, and $T_{din}(t)$ is the dynamic effective tension at the TDP. Thus, s_{TDP} is the s at the static TDP and $x_0(t)$ is given by

$$x_0(t) = -\frac{T_{ef,0}}{\gamma_{ef}}\theta(s_{TDP},t)$$

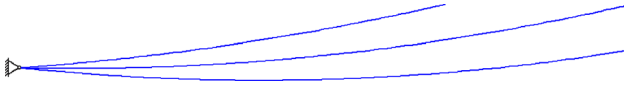

Fig. 2 Sketch of the frequency domain's boundary condition. The middle position is the static configuration and the other two are dynamic instants.

Table 1 Catenary's properties

	Segment 1
Diameter (m)	0.4064
Weight in air (kN/m)	2.4927
Bending stiffness (kN m^2)	78,000
Axial stiffness (kN)	4,000,000
Torsional stiffness (kN m^2)	60,000
Length (m)	4440
Drag coefficient	1.1
Inertia coefficient	2

where $\theta(s_{TDP}, t)$ is obtained through the frequency domain analysis with the articulated joint at the TDP and γ_{ef} is the effective weight per unit of the length of the riser.

According to this model, there is a peak of the dynamic amplitude of the curvature that occurs in $s = s_{TDP} + x_0(t)$, the farthest section from the TDP for which the condition $\beta_{CL}(s,t) \leq 0$ occurs.

4 Frequency Domain Solution

Considering that all the nonlinearities have been removed and that the excitation is harmonic, the equation of motion can be written as

$$M\ddot{q}(t) + C\dot{q}(t) + Kq(t) = p_0 e^{i\omega t} \tag{12}$$

and the displacement can be written as

$$q(t) = q_0 e^{i\omega t} \tag{13}$$

Thus, the first and the second derivatives of the displacements are

$$\dot{q}(t) = i\omega\, q_0 e^{i\omega t} \tag{14}$$

$$\ddot{q}(t) = -\omega^2 q_0 e^{i\omega t} \tag{15}$$

Therefore, Eq. (13) can be rewritten as

$$(-\omega^2 M + i\omega C + K) q_0 e^{i\omega t} = p_0 e^{i\omega t} \tag{16}$$

Defining the dynamic matrix D as

$$D = -\omega^2 M + i\omega C + K \tag{17}$$

it can be replaced in Eq. (17) to obtain

$$D \cdot q_0 = p_0 \tag{18}$$

Equation (18) shows that to solve the problem in the frequency domain corresponds to solving a system of linear algebraic equations. Nevertheless, this system has to be solved several times, because of the linearization of the damping. Since the riser velocity is not known at the beginning of the analysis, the linearization factor is iteratively obtained, which means that the matrix C changes in each iteration and, consequently, the matrix D changes as well. The stop criteria, used in this work, considers that the relative difference of the amplitude of each node's movement is smaller than a given precision.

Table 2 Lazy-wave's properties

	Segment 1	Segment 2	Segment 3
Diameter (m)	0.4064	0.8	0.4064
Weight in air (kN/m)	2.4927	3.9044	2.4927
Bending stiffness (kN m^2)	78,000	78,000	78,000
Axial stiffness (kN)	4,000,000	4,000,000	4,000,000
Torsional stiffness (kN m^2)	60,000	60,000	60,000
Length (m)	2800	400	1200
Drag coefficient	1.1	1.1	1.1
Inertia coefficient	2	2	2

Table 3 Geometrical and environmental data

Geometry	X_{top} (m)	3800
	Z_{top} (m)	1255
Environment	Depth (m)	1255
	Water density (t/m^3)	1.024
	Gravity acceleration (m/s^2)	9.807

5 Case Study

The case study consists of the same steel riser in two different configurations. The first configuration is a steel catenary riser with 16 in. of external diameter and 1 in. of thickness. The properties can be found in Table 1.

The second configuration is a steel lazy-wave with the properties presented in Table 2.

The environmental and geometrical data for this analysis can be found in Table 3.

Table 4 shows the wave and motion that is prescribed in the floating unit. It is considered that the riser is installed in a floating production storage and offloading (FPSO) and subjected to a typical centenary wave in the Campos Basin, presented in DNV-OS-E301 [20].

Not surprisingly, for the catenary riser, these movements caused dynamic compression, as shown in Fig. 3. This figure shows the effective tension comparison between Orcaflex^{TM} and the frequency domain (FD).

Therefore, in order to compare the methodology, half of the movements and wave height were considered in the catenary simulation.

There are some locations, however, where typical centenary waves are higher than the waves on the Brazilian coast. To test the presented model, the highest wave suggested in DNV-OS-E301 [20] is also simulated, keeping the other conditions the same. The chosen wave is a Norwegian sea wave and its data and the corresponding to the top movement can be seen in Table 5.

For all of the cases, the current profile is the same and can be seen in Table 6.

According to DNV-RP-F105 [21], the friction coefficient $\mu = 0.2$ may be applied for span supports on sand and $\mu = 0.6$ may be applied for span supports on clay. For the examples in this paper, a value between them $\mu = 0.4$ was chosen.

6 Results

The precision considered in the frequency domain analyses was 0.01% and the parameter considered for the convergence was the nodal movement. Table 7 shows the number of iterations until convergence of frequency domain analyses presented in this paper.

The results of all analyses compared to the results obtained with Orcaflex^{TM}, which performs a full nonlinear analysis, are shown in Figs. 4, 5, and 6.

Table 4 Wave and top motion for the Campos Basin

	Period	13.0 s
Wave	Height	8.0 m
	Angle	90 deg
X Movement	Amplitude	1.601 m
	Phase	75.8112 deg
Y Movement	Amplitude	1.3383 m
	Phase	−14.9582 deg
Z Movement	Amplitude	4.9996 m
	Phase	58.9947 deg

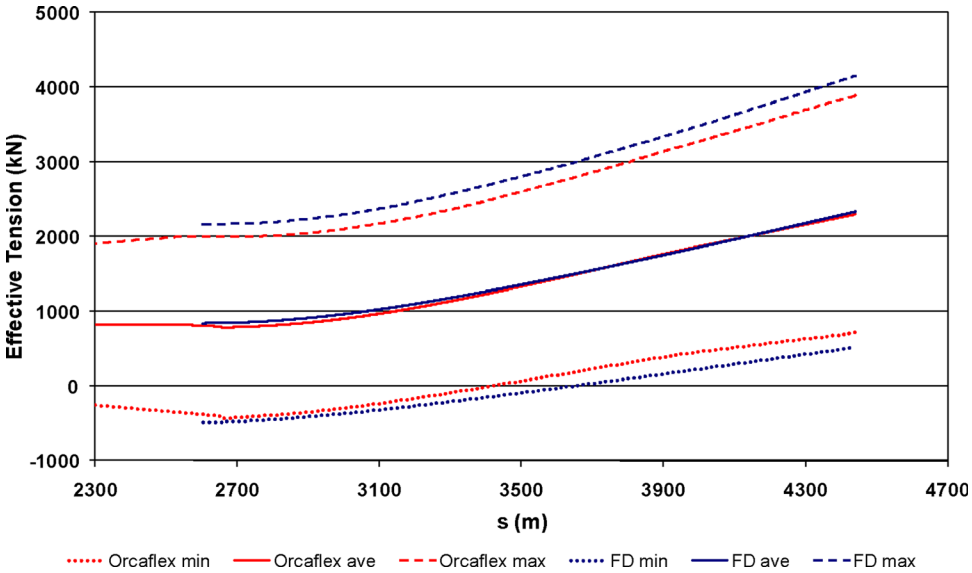

Fig. 3 Effective tension envelope comparison for the catenary. Min denotes the minimum values, ave denotes average, and max denotes the maximum values.

They show the X, Y, Z, θ, ψ, out-of-plane curvature, in-plane curvature, and the effective tension amplitudes in the function of the curvilinear coordinate s. ["The in-plane direction is normal to both the line's axis (at the specified arc length) and the vertical direction. The out-of-plane direction is normal to both the line's axis and the in-plane direction." (see the Orcaflex Manual [1], page 308)]. In both figures, the FD represents the frequency domain results and BL represents the boundary layer results.

Since only the static suspended part of the riser was simulated in the frequency domain analysis, the figures show Orcaflex's results for the whole riser compared to the suspended part of the riser in the frequency domain.

The boundary condition considered at the TDP was: X, Y, and Z translations fixed and free to rotate. Analyzing this in Figs. 4, 5, and 6, a small movement can be seen in the X and Y amplitudes at the TDP region, which shows that fixing the static TDP was a good approach. The free rotation can be seen in the θ and ψ angle comparisons. An amplitude of θ at the TDP can be seen, but Orcaflex's results start from zero and increases approximately to the value calculated in the frequency domain. A different behavior can be seen in the ψ angle: the amplitude is small at the TDP region, probably because of the friction between the riser and the seabed.

The out-of-plane curvature presents a peak at the TDP region. The peak was recovered by the frequency domain analysis, however, its position is a slightly different, since only the suspended part of the riser is simulated.

Generally, the shape and the values of the amplitudes were recovered, and only small differences can be seen. The boundary layer technique recovered the peak of the in-plane curvature in the TDP region and also its position for all cases. The value of the effective tension is zero on the part of the segment of the riser that is in contact with the seabed. That is caused by the friction. However, that part is not simulated in the frequency domain analysis.

The aim of the model presented here is not to simulate the dynamic compression that is the reason that the prescribed movement for the catenary riser was changed. However, the effective tension comparison in Fig. 3 shows that the frequency domain model can predict when part of the riser is under dynamic compression.

7 Conclusion

This paper addressed the dynamic analysis of risers in the frequency domain. More precisely, it presented a method of linearization to treat the nonlinearities inherent to the analysis in order to make it viable to perform it in the frequency domain with harmonic seas.

Table 5 Wave and top motion for the Norwegian Sea

	Period	17 s
Wave	Height	16.5 m
	Angle	90 deg
X Movement	Amplitude	1.8209 m
	Phase	39.5992 deg
Y Movement	Amplitude	8.2521 m
	Phase	−87.9111 deg
Z Movement	Amplitude	9.7943 m
	Phase	−43.701 deg

Table 6 Current profile

Depth (m)	Velocity (m/s)	Angle (deg)
1255	0	135
1254.5	0	135
915	0.66	135
750	0.69	135
640	0.48	135
545	0.39	135
415	0.6	45
340	0.64	0
230	0.67	0
140	1.1	0
100	1.29	0
50	1.43	0
0	1.8	0

Table 7 Number of iterations until convergence of the frequency domain analyses

Catenary in the Campos Basin	14 iterations
Catenary in the half wave of Campos Basin	42 iterations
Lazy-wave in the Campos Basin	27 iterations
Lazy-wave in the Norwegian Sea	23 iterations

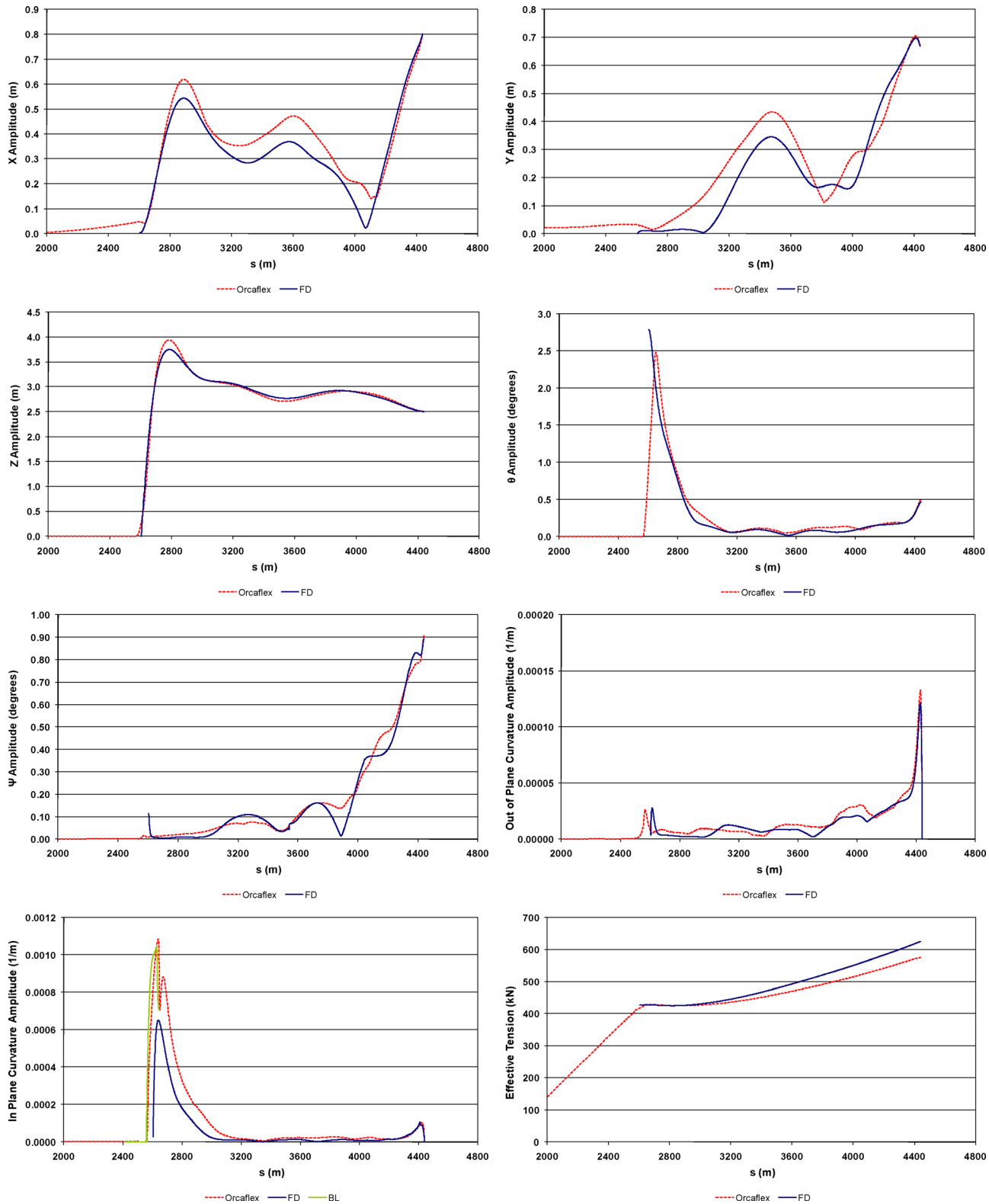

Fig. 4 Results of the catenary in the half wave of the Campos Basin. They show the X, Y, Z, θ, ψ, out-of-plane curvature, in-plane curvature, and effective tension amplitudes in the function of the curvilinear coordinate *s*. BL denotes the boundary layer results.

First, the dynamics of the riser were considered to be a perturbation of the static configuration. It means that the static angles and loads are used to obtain the elements' matrices that will constitute the global mass, damping, stiffness matrices, and load vector. This implies that the static configuration is the mean configuration around which the riser moves.

The viscous part of Morison's formula is generally used to obtain the damping matrix of the risers. However, it quadratically depends on the relative velocity. An iterative method has been presented in this paper to deal with this problem. It is an extension of the method presented in Takafuji and Martins [16], aiming to perform the analysis in threedimensions. Globally, the obtained

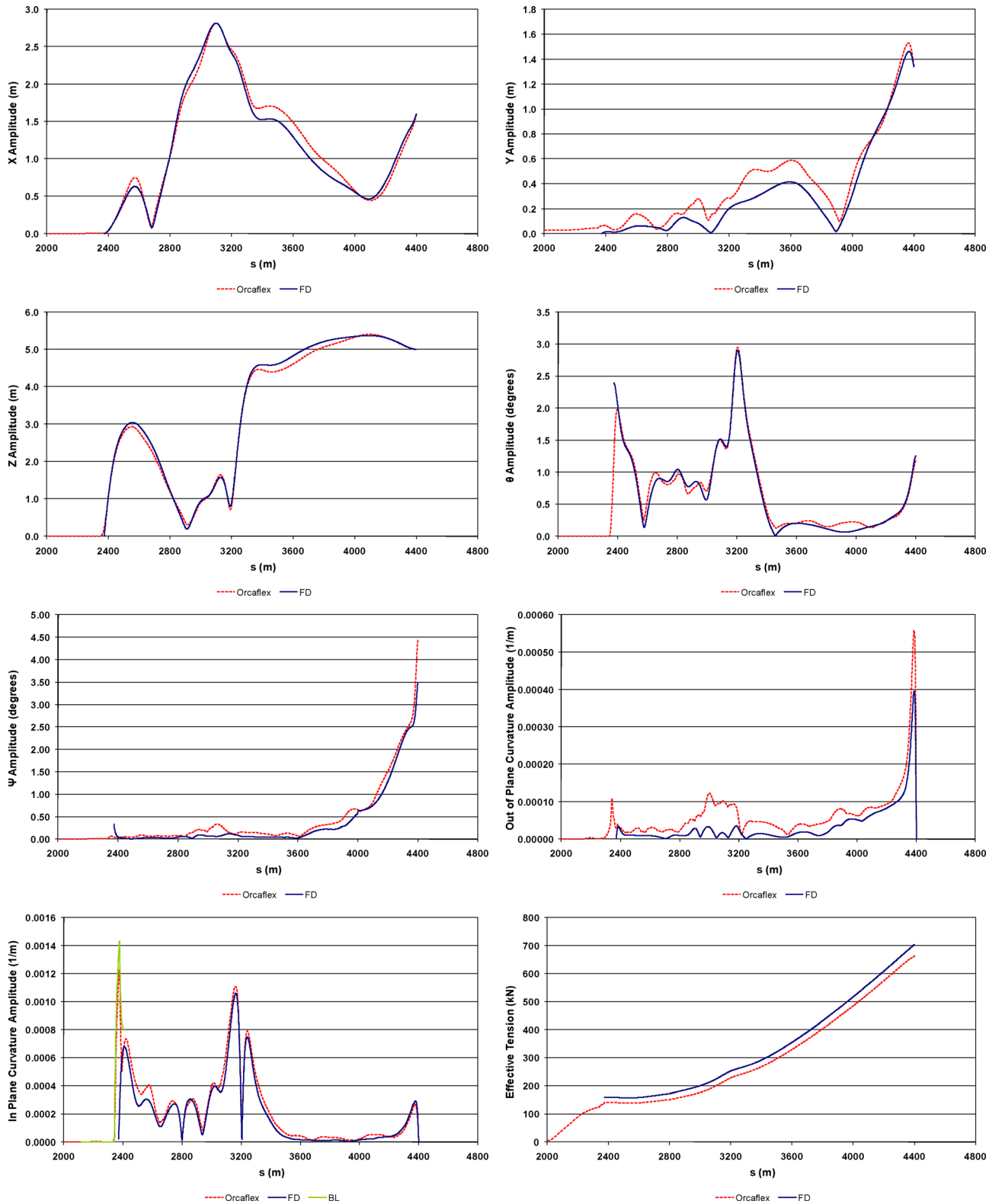

Fig. 5 Results of the lazy-wave in the Campos Basin. They show the X, Y, Z, θ, ψ, out-of-plane curvature, in-plane curvature, and effective tension amplitudes in the function of the curvilinear coordinate *s*. BL denotes the boundary layer results.

results were good. They show that this iterative method is a good option for damping linearization in the frequency domain analysis. The iterative process was necessary to take into account, as closely as possible, the nonlinearity caused by Morison's formula.

Another nonlinearity treated for the frequency domain analysis was the riser-seabed contact. Only the suspended part of the riser is simulated. The movements seen in the X and Y amplitudes at the TDP region are small, and fixing the model at the static TDP was a good approach. However, an idea to recover the movements is to use horizontal springs at that position, instead of using a pinned support. The springs could also improve the results of the ψ angle at the TDP region.

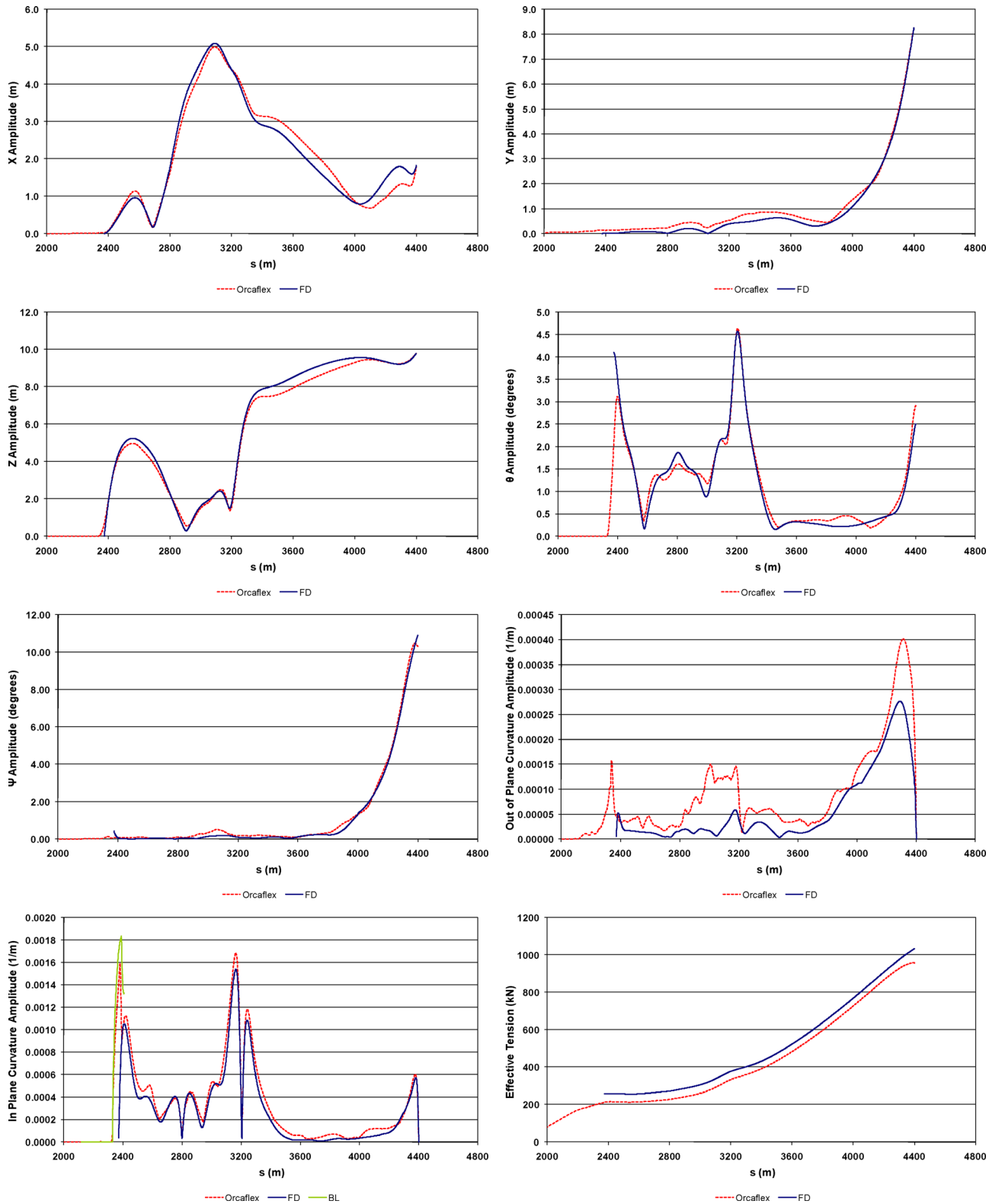

Fig. 6 Results of the lazy-wave in the Norwegian Sea. They show the X, Y, Z, θ, ψ, out-of-plane curvature, in-plane curvature, and effective tension amplitudes in the function of the curvilinear coordinate *s*. BL denotes the boundary layer results.

The in-plane curvature was corrected afterwards through a boundary layer technique, because the unilateral contact was removed. In general, the boundary layer technique recovered the height of curvature's peak and its position at the TDP region.

Although there are some differences, comparing the overall results obtained in frequency domain with the ones obtained with a full nonlinear in time domain, one can see that the frequency domain analysis is viable. It is important to know its limitations and the hypotheses behind the analysis. Nonetheless, due to the time it takes to perform, it is viable to use the frequency domain analysis, especially in the first stages of a riser design, when a large amount of simulations are required.

References

[1] Orcina, 2010, "OrcaFlex Manual Version 9.4a," Daltongate, Ulverston, Cumbria, UK.

[2] Patel, M. H., and Seyed, F. B., 1995, "Review of Flexible Riser Modelling and Analysis Techniques," Eng. Struct., **17**(4), pp. 293–304.

[3] Santos, M. F., 2003, "Three-Dimensional Global Mechanics of Submerged Cables," PhD thesis, University of Sao Paulo, Sao Paulo, Brazil (in Portuguese).

[4] Silveira, L. M. Y., and Martins, C. A., 2004, "A Numerical Method to Solve the Static Problem of a Catenary Riser," Proceedings of the 23rd International Conference on Offshore Mechanics and Arctic Engineering (OMAE), Canada.

[5] Silveira, L. M. Y., and Martins, C. A., 2005, "A Numerical Method to Solve the Three-Dimensional Static Problem of a Riser With Bending Stiffness," Proceedings of the 24th International Conference on Offshore Mechanics and Arctic Engineering (OMAE), Greece.

[6] Aranha, J. A. P., Martins, C. A., and Pesce, C. P., 1997, "Analytical Approximation for the Dynamic Bending Moment at the Touchdown Point of a Catenary Riser," Int. J. Offshore Polar Eng., **7**(4), pp. 293–300.

[7] Keller, H. B., 1968, *Numerical Methods for Two-Point Boundary Value Problems*, Blaisdell, Waltham, MA.

[8] Martins, C. A., 1998, "Poliflex – Poliflex User's Manual," EPUSP, São Paulo (in Portuguese).

[9] Morison, J. R., O'Brian, M. P., Johnson, J. W., and Schaaf, S. A., 1950, "The Force Exerted by Surface Waves on Piles," Trans. Am. Inst. Min., Metall. Pet. Eng., **189**, pp. 149–154.

[10] Dantas, C. M. S., Siqueira, M. Q., Ellwanger, G. B., Torres, A. L. F. L., and Mourelle, M. M., 2004, "A Frequency Domain Approach for Random Fatigue Analysis of Steel Catenary Risers at Brazil's Deep Waters," Proceedings of the 23rdInternational Conference on Offshore Mechanics and Arctic Engineering (OMAE), Canada.

[11] Gudmestad, O. T., and Connor, J. J., 1983, "Linearization Methods and the Influence of Current on the Nonlinear Hydrodynamic Drag Force," Appl. Ocean Res., **5**(4), pp. 184–194.

[12] Langley, R. S., 1984, "The Linearisation of Three Dimensional Drag Force in Random Seas With Current," Appl. Ocean Res., **6**(3), pp. 126–131.

[13] Leira, B. J., 1987, "Multidimensional Stochastic Linearisation of Drag Forces," Appl. Ocean Res., **9**(3), pp. 150–162.

[14] Chen, Y. H., and Lin, F. M., 1989, "General Drag-Force Linearization for Nonlinear Analysis of Marine Risers," Ocean Eng., **16**(3), pp. 265–280.

[15] Liu, Y., and Bergdahl, L., 1997, "Frequency-domain Dynamic Analysis of Cables," Eng. Struct., **19**(6), pp. 499–506.

[16] Martins, C. A., 2000, "A Tool to the Viability Study of Steel Catenary Risers," Habilitation thesis, University of Sao Paulo, Sao Paulo, Brazil (in Portuguese).

[17] Takafuji, F. C. M., and Martins, C. A., 2007, "Damping Linearization for Frequency Domain Lazy-Wave Riser Analysis," Proceedings of the 17th International Offshore and Polar Engineering Conference, Lisbon, Portugal.

[18] Takafuji, F. C. M., 2010, "Three-Dimensional Riser Dynamics," PhD thesis, University of Sao Paulo, Sao Paulo, Brazil (in Portuguese).

[19] Teng, B., and Li, Y. C., 1990, "The Linearization of Drag Force and the Error Estimation of Linear Force Spectrum," Coastal Eng., **14**, pp. 173–183.

[20] Det Norsk Veritas, 2010, "Position Mooring," Recommended Practice Report No. DNV-OS-E301.

[21] Det Norsk Veritas, 2006, "Free Spanning Pipelines," Recommended Practice Report No. DNV-RP-F105.